Analysis of Corrugated Long-Period Gratings in Slab Waveguides and Their Polarization Dependence

Qing Liu, *Student Member, IEEE*, Kin Seng Chiang, *Member, IEEE, Fellow, OSA*, and Vipul Rastogi, *Member, IEEE, Member, OSA*

***Abstract*—We analyze theoretically the light transmission characteristics of corrugated long-period gratings formed in slab waveguides. The transmission spectra of the gratings show distinct rejection bands at specific wavelengths, known as the resonance wavelengths. We investigate in detail the phase-matching curves of the gratings, which govern the relationship between the resonance wavelength and the grating period. Thanks to the flexibility in the choice of the waveguide parameters, the phase-matching curves of a long-period waveguide grating can be different characteristically from those of a long-period fiber grating (LPFG), which implies that the former can exhibit much richer characteristics than the latter. Unlike an LPFG, the transmission spectrum of a long-period waveguide grating is in general sensitive to the polarization of light. Nevertheless, a proper choice of the waveguide and grating parameters can result in a polarization-independent rejection band. Long-period waveguide gratings should find potential applications in a wide range of integrated-optic waveguide devices and sensors.**

***Index Terms*—Coupled-mode analysis, gratings, optical filters, optical planar waveguides, optical polarization, optical waveguide filters, optical waveguides.**

I. Introduction

In recent years, significant efforts have been directed into the development of long-period fiber gratings (LPFGs) for gain equalizing or flattening of erbium-doped fiber amplifiers (EDFAs) [1]–[4], multichannel filtering in wavelength-division multiplexed systems [5], [6], and various sensing applications [7]–[10]. An LPFG written in a single-mode fiber is capable of coupling light from the fundamental mode to selected cladding modes at specific wavelengths [1]. This results in a transmission spectrum with a number of rejection bands. In comparison with fiber Bragg gratings (FBGs), LPFGs offer a number of advantages, including easy fabrication, low back reflection, and better wavelength tunability. These advantages render the LPFG particularly desirable for applications where a narrow bandwidth is not required. Detailed theoretical analyses of the transmission characteristics of LPFGs are available (see, for example, [11] and references therein).

It has been demonstrated that many of the characteristics of LPFGs can be controlled effectively by using special fiber designs [12]–[15] or by etching the fiber diameter [16], [17]. However, the geometry and material constraints of a fiber still impose significant limitations on the functions that an LPFG can achieve, especially on the realization of active devices. To remove the constraints of a fiber, long-period waveguide gratings (LPWGs) have been proposed [18], [19]. Recently, widely tunable corrugated LPWG filters in polymer-coated glass waveguides [20] have been demonstrated experimentally, which provide linear wavelength tuning over the entire C+L band (~90 nm) with a temperature control of only ~ 10 °C. These filters outperform the reported tunable LPFG filters [14], [15] on both wavelength tuning range and sensitivity.

In this paper, we present a theoretical analysis of corrugated LPWGs in slab waveguides. In particular, we calculate the transmission spectra for both the TE and TM polarizations, investigate the effects of the waveguide cladding on the phase-matching curves, and highlight the possibility of achieving polarization-insensitive rejection bands. This paper extends substantially the previous work, where a phase LPWG in a slab waveguide with a thick cladding for the TE polarization is considered [18]. This paper shows that, as the cladding of the waveguide becomes thin, the transmission properties of an LPWG can change markedly. Furthermore, corrugation is a more universal approach for the fabrication of waveguide gratings. Our results should provide a better understanding of the properties of an LPWG, as well as useful guidance for the design of LPWG-based devices.

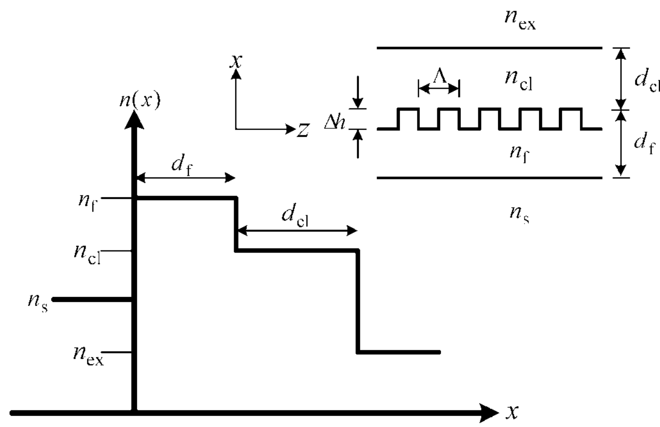

Fig. 1. Refractive-index profile of a four-layer planar waveguide, where a corrugated long-period grating is introduced on the surface of the guiding layer.

II. Method of Analysis

Fig. 1 shows a four-layer slab waveguide structure, which consists of a substrate of refractive index n_s, a guiding layer of refractive index n_f and thickness d_f, a cladding layer of refractive index n_{cl} and thickness d_{cl}, and an external medium of re-

Manuscript received June 23, 2003; revised September 4, 2003. This work was supported by the Research Grants Council of the Hong Kong Special Administrative Region, China, under Project . CityU 1160/01E.

The authors are with the Optoelectronics Research Centre and Department of Electronic Engineering, City University of Hong Kong, Hong Kong, China (e-mail: eeksc@cityu.edu.hk).

Digital Object Identifier 10.1109/JLT.2003.821749

fractive index $n_{\rm ex}$ that extends to infinity, where $n_{\rm f} > n_{\rm cl} > n_{\rm s}$, $n_{\rm ex}$. We assume that only the fundamental $\rm TE_0$ and $\rm TM_0$ modes are guided with $n_{\rm cl} < N_0 < n_{\rm f}$, where N_0 is the mode index, and a corrugated grating with period Λ and corrugation depth Δh is introduced on the surface of the guiding layer. The grating allows light coupling from the fundamental mode ($\rm TE_0$ or $\rm TM_0$) to the cladding ($\rm TE_m$ or $\rm TM_m$) modes whose mode indexes $N_m (m = 1, 2, 3, \ldots)$ are smaller than $n_{\rm cl}$, i.e., $n_{\rm s} < N_m < n_{\rm cl}$.

The transmission characteristics of the LPWG can be analyzed by the coupled-mode theory [1], [18]. The resonance wavelength λ_0, namely, the wavelength at which the coupling between the fundamental mode and the mth order cladding mode is strongest, is obtained as

$$\lambda_0 = (N_0 - N_m)\,\Lambda \tag{1}$$

which is referred to as the phase-matching condition. In general, the resonance wavelengths for the TE and TM polarizations are different. The transmission coefficient at any wavelength λ is given by

$$T = 1 - \frac{\kappa^2}{\kappa^2 + \frac{\delta^2}{4}} \sin^2 \sqrt{\kappa^2 + \frac{\delta^2}{4}}\, L \tag{2}$$

where $\delta = (2\pi/\lambda)(N_0 - N_m) - 2\pi/\Lambda = (2\pi/\Lambda)(\lambda_0 - \lambda)/\lambda$ is a detuning parameter (phase mismatch) that measures the deviation of the wavelength λ from λ_0, κ is the coupling coefficient, and L is the length of the grating. For the grating shown in Fig. 1, the coupling coefficient κ arises from the corrugation along the guiding layer of the waveguide and, in general, depends on the polarization of light. According to the coupled-mode theory [21], the grating is treated as a perturbation of a uniform waveguide with guiding layer thickness $d_{\rm f} - \Delta h/2$ and cladding thickness $d_{\rm cl} + \Delta h/2$, as shown in Fig. 1. By following the procedures detailed in [21] and considering only the first spatial harmonic of the grating, we obtain the general expressions for the coupling coefficient of the LPWG. For the TE polarization, the coupling coefficient, denoted as $\kappa_{\rm TE_0 \to TE_m}$, is given by

$$\kappa_{\rm TE_0 \to TE_m} = \frac{k_0 \Delta n_0^2}{2\pi c \mu_0} \int_{d_{\rm f} - \Delta h}^{d_{\rm f}} E_{0y} E_{my}\, dx \tag{3}$$

where c is the speed of light in vacuum, μ_0 is the magnetic permeability, $\Delta n_0^2 = n_{\rm f}^2 - n_{\rm cl}^2$, $k_0 = 2\pi/\lambda$ is the wave-number, and E_{0_y} and E_{my} are the normalized electric fields (along the y-direction) for the $\rm TE_0$ and $\rm TE_m$ modes, respectively. For the TM polarization, the coupling coefficient, denoted as $\kappa_{\rm TM_0 \to TM_m}$, is given by

$$\kappa_{\rm TM_0 \to TM_m} = \kappa_x + \kappa_z \tag{4}$$

with

$$\kappa_x = \frac{k_0 \Delta n_0^2 N_0 N_m}{2\pi c \varepsilon_0 n_{\rm f}^2 n_{\rm cl}^2} \times \left(\frac{n_{\rm cl}^2}{n_{\rm f}^2} \int_{d_{\rm f} - \Delta h}^{d_{\rm f} - \Delta h/2} H_{0y} H_{my}\, dx + \frac{n_{\rm f}^2}{n_{\rm cl}^2} \int_{d_{\rm f} - \Delta h/2}^{d_{\rm f}} H_{0y} H_{my}\, dx \right)$$

$$\kappa_z = \frac{\Delta n_0^2}{2\pi c \varepsilon_0 k_0 n_{\rm f}^2 n_{\rm cl}^2} \int_{d_{\rm f} - \Delta h}^{d_{\rm f}} \frac{\partial H_{0y}}{\partial x} \frac{\partial H_{my}}{\partial x}\, dx \tag{5}$$

where ε_0 is the electric permeability of vacuum and H_{0_y} and H_{my} are the normalized magnetic fields (along the y-direction) for the $\rm TM_0$ and $\rm TM_m$ modes, respectively. The result for the TM polarization is more complicated, because the TM mode consists of two electric field components, one along the x-direction and the other along the z-direction, and the x-component is discontinuous at the waveguide boundaries. On the other hand, the TE mode contains only one electric field component along the y-direction, which is continuous everywhere. By substituting the appropriate mode fields in (3)–(5), the coupling coefficients, and hence, the transmission coefficients, can be evaluated. For a four-layer slab waveguide, analytical eigenvalue equations for solving the mode indexes and the mode fields are available (see, for example, [22]). The mode fields are normalized according to $-(1/2){\rm Re} \int_{-\infty}^{\infty} E_y H_x^* dx = 1$ for the TE modes and $(1/2){\rm Re} \int_{-\infty}^{\infty} H_y E_x^* dx = 1$ for the TM modes, where the subscript denotes the direction of the field component.

For all the numerical results given in subsequent sections, unless stated otherwise, the following waveguide parameters are used: $n_{\rm s} = 1.444$, $n_{\rm f} = 1.53$, $n_{\rm cl} = 1.50$, $n_{\rm ex} = 1.0$ (air), and $d_{\rm f} = 2.0$ μm. These values are typical of a polymer waveguide fabricated on a silica substrate. The cladding thickness $d_{\rm cl}$, which is an important design parameter, is allowed to vary. For the sake of simplicity, material dispersion and stress-induced birefringence are ignored in the analysis, although they can be readily incorporated into the analysis if their values are known.

III. Phase-Matching Curves

The phase-matching condition given by (1) governs the dependence of the resonance wavelength on the pitch of the grating and, therefore, plays a central role in the study of long-period gratings.

The variation of the resonance wavelength with the grating pitch is shown in Fig. 2 for four different values of cladding thickness: $d_{\rm cl} = 10$ μm, 5 μm, 2 μm, and 1 μm. The curves shown in Fig. 2 are referred to as the phase-matching curves, which help us choose a grating period to filter out a certain wavelength from the transmission spectrum of the waveguide. Each curve characterizes the coupling between the fundamental mode and a particular cladding mode.

When the cladding is thick, as shown in Fig. 2(a), the number of cladding modes available for light coupling decreases as the grating period increases. The slope of the curve for a high-mode order, e.g., $m = 3$ or 4 in Fig. 2(a), changes sign from positive to negative as the wavelength increases. In other words, the curve exhibits a turning point, which implies that two resonance wavelengths that correspond to the same cladding mode can be produced with the same grating period. The turning point occurs at a longer wavelength for a lower order mode; it shifts to a shorter wavelength as the mode order increases. As a matter of fact, dual resonance wavelengths have been observed in an LPFG for a high-order cladding mode (e.g., the $\rm LP_{015}$ mode) [23]. Our results show clearly that dual resonance wavelengths should be observable with a relatively low-order mode in an LPWG.

It is noted that the phase-matching curves for the TE and TM polarizations are in general different. To facilitate the discussion

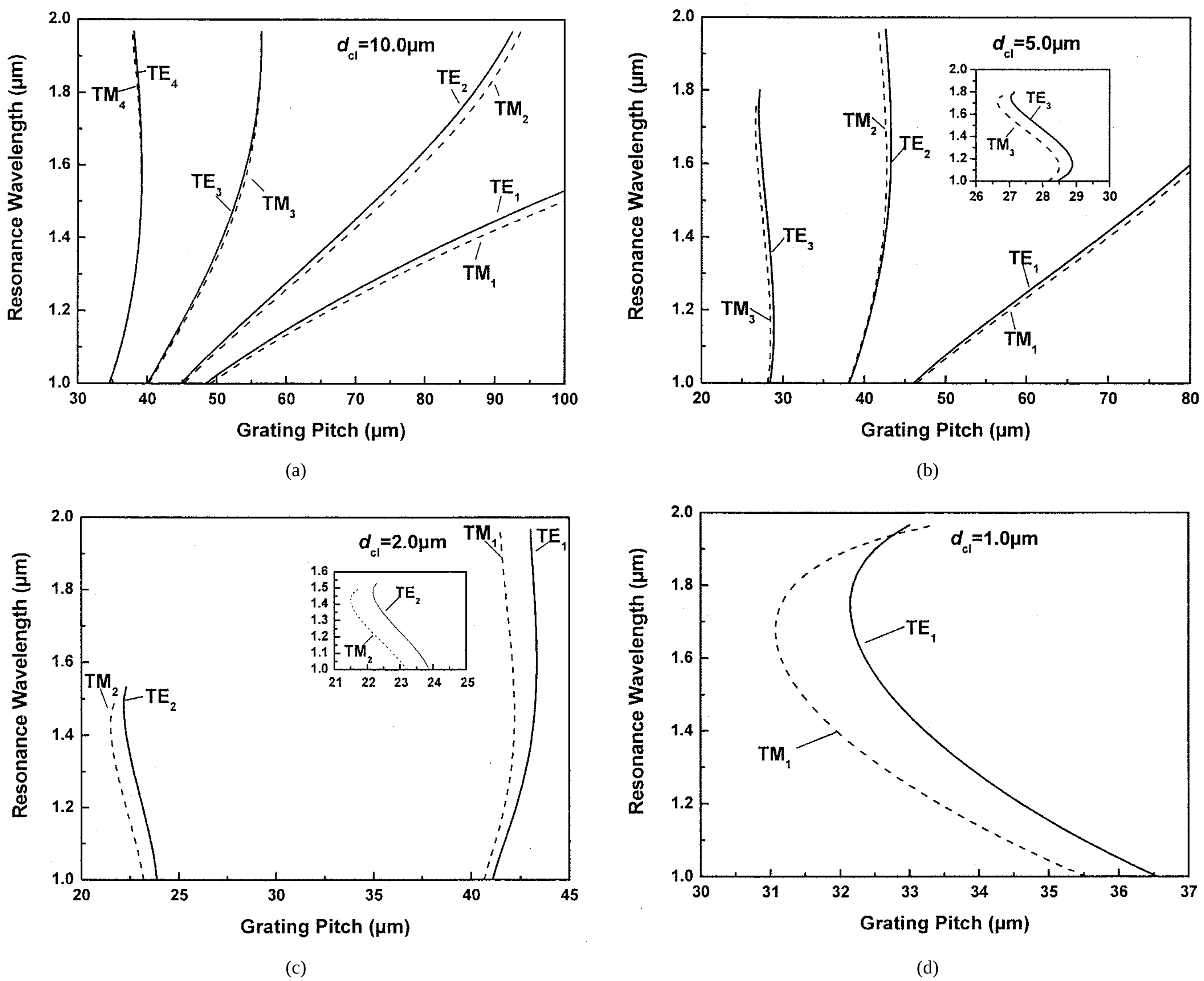

Fig. 2. Phase-matching curves for an LPWG with $n_s = 1.444$, $n_f = 1.53$, $n_{cl} = 1.50$, $n_{ex} = 1.0$, and $d_f = 2.0$ μm at different values of cladding thickness: (a) $d_{cl} = 10.0$ μm, (b) $d_{cl} = 5.0$ μm, (c) $d_{cl} = 2.0$ μm, and (d) $d_{cl} = 1.0$ μm.

of this property, we propose a waveguide parameter D_m, which is defined as

$$D_m = \left(N_0^{\mathrm{TE}} - N_m^{\mathrm{TE}}\right) - \left(N_0^{\mathrm{TM}} - N_m^{\mathrm{TM}}\right), \quad \text{for } m = 1, 2, \ldots \tag{6}$$

where the superscript labels the polarization associated with the mode index. Clearly, according to (1), D_m is a measure of the difference between the resonance wavelengths of the TE and TM polarizations. As shown in Fig. 2(a), D_1 and D_2 are always positive, i.e., the TE modes couple at a longer wavelength than the TM modes. However, for the higher order modes ($m = 3$ and 4), the TE and TM phase-matching curves become close and, in fact, can cross each other, i.e., D_3 and D_4 can change sign. This implies the presence of a specific grating period that can bring D_3 or D_4 to zero, so that the couplings for both polarizations occur at the same wavelength.

As the cladding thickness decreases, the number of cladding modes supported by the waveguide decreases. For the present waveguide, only one cladding mode exists when the cladding thickness is reduced to 1 μm. As shown by the results in Fig. 2(b)–(d), the dual resonance phenomenon can be observed with even the first-order cladding modes (TE_1 and TM_1 modes), if the cladding is thin enough. Our finding extends the knowledge of an LPFG. Because the fiber cladding is thick (62.5 μm in radius), dual resonance occurs only at a high cladding mode order in an LPFG [23]. Here we find that the cladding mode order for such a phenomenon to occur actually decreases with the cladding thickness. It should be easy to observe dual resonance with an LPWG by using a thin cladding.

In the case of an LPFG, because the fiber cladding is large, a small change in the cladding thickness affects only the mode indexes of the cladding modes. Although a fiber cladding as thin as 34.8 μm in radius has been demonstrated [16], it is still considered thick, compared with that used in a waveguide. In the case of an LPWG, because the cladding is much thinner, a change in the cladding thickness can affect not only the mode indexes of the cladding modes but also the mode index of the guided mode. This can give rise to phase-matching curves that are markedly different from those for an LPFG. In particular, multiple resonance wavelengths at a given grating period, as calculated from

(1), become possible over a narrow range of wavelengths, as shown in Fig. 2. While the phase-matching curves for the case $d_{\text{cl}} = 10\ \mu\text{m}$, as shown in Fig. 2(a), still resemble those of an LPFG, the curves for the cases $d_{\text{cl}} = 5\ \mu\text{m}$, 2 μm, and 1 μm, as shown in Fig. 2(b)–(d), show characteristically different features. For the case $d_{\text{cl}} = 1\ \mu\text{m}$, the phase-matching curve for the TE_1 (or TM_1) mode actually starts with a positive slope at a short wavelength and turns back at a longer wavelength (not shown in the figure) with a negative slope. It turns back again at an even longer wavelength (1.7–1.8 μm) with a positive slope. Fig. 2(d) shows only the second turning point of the curve. The same features can be seen in Fig. 2(c) for the TE_2 and TM_2 modes, and in Fig. 2(b) for the TE_3 and TM_3 modes.

The slope of the phase-matching curve $d\lambda_0/d\Lambda$ depends on the dispersion characteristics of the guided mode and the cladding mode of concern [24]. For an LPFG, it has been shown that this parameter governs the sensitivity of the resonance wavelength to any physical parameter, which can be an environmental parameter, such as temperature, strain, pressure, surrounding refractive index, etc., or a fiber parameter such as the cladding radius [25]. Since the phase-matching curves of an LPWG can be markedly different from those of an LPFG, we expect that the sensitivity characteristics of an LPWG can also be markedly different from those of an LPFG. By removing the geometry and material constraints of an LPFG, much richer transmission characteristics can be achieved with an LPWG.

IV. Coupling Coefficients

According to (2), the strength of the rejection band of an LPWG is governed by the coupling coefficient. Fig. 3 shows the coupling coefficients for the TE_0–TE_1 and TM_0–TM_1 couplings as functions of the corrugation depth Δh for $d_{\text{cl}} = 4\ \mu\text{m}$ and $\lambda_0 = 1.584\ \mu\text{m}$. Because the electric and magnet fields depend on the corrugation depth, the coupling coefficients as given by (3)–(5) can be expanded in terms of $\Delta h, \Delta h^2, \Delta h^3, \ldots$. When Δh is small, the higher order terms in the expansions can be neglected and the coupling coefficients increase linearly with the corrugation depth. When Δh is large, however, the higher order terms become significant and the relationship between the coupling coefficient and the corrugation depth is no longer linear, as shown in Fig. 3.

The results in Fig. 3 help us choose a suitable corrugation depth to achieve a specific contrast for a given grating length. For example, with $L = 4$ mm, the coupling coefficient required for achieving a maximum contrast is given by $\kappa = \pi/2L \cong 3.9 \times 10^{-4}\ \mu\text{m}^{-1}$, which, according to Fig. 3, requires a corrugation depth of ~90 nm (~4.5% of the thickness of the guiding layer) for the TE polarization. On the other hand, for an LPFG to give a similar performance, a grating length of several centimeters is usually required [1]–[10]. Corrugation is an effective means for making strong gratings.

The dependence of the coupling coefficient on the cladding thickness is shown in Fig. 4 for several cladding modes (assuming $\Delta h = 0.1\ \mu\text{m}$ and $\lambda_0 = 1.584\ \mu\text{m}$). It is seen from Fig. 4 that the coupling coefficient increases with the cladding thickness initially and reaches a maximum value at a particular cladding thickness. It then decreases with a further increase in the cladding thickness. When the cladding becomes thick enough, the coupling coefficient can change sign. All these features are the results of modifying the mode field distributions in the waveguide as the cladding thickness changes. As shown in Fig. 4, for the same mode order, the coupling coefficient for the TE polarization is generally larger than that for the TM polarization.

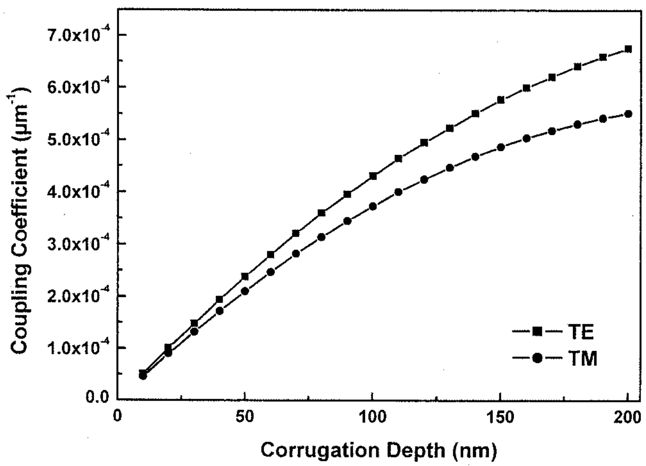

Fig. 3. Dependence of the coupling coefficients for the TE_0–TE_1 and TM_0–TM_1 couplings on the corrugation depth Δh for an LPWG with $n_s = 1.444$, $n_f = 1.53$, $n_{\text{cl}} = 1.50$, $n_{\text{cx}} = 1.0$, $d_f = 2.0\ \mu\text{m}$, $d_{\text{cl}} = 4\ \mu\text{m}$, and $\lambda_0 = 1.584\ \mu\text{m}$.

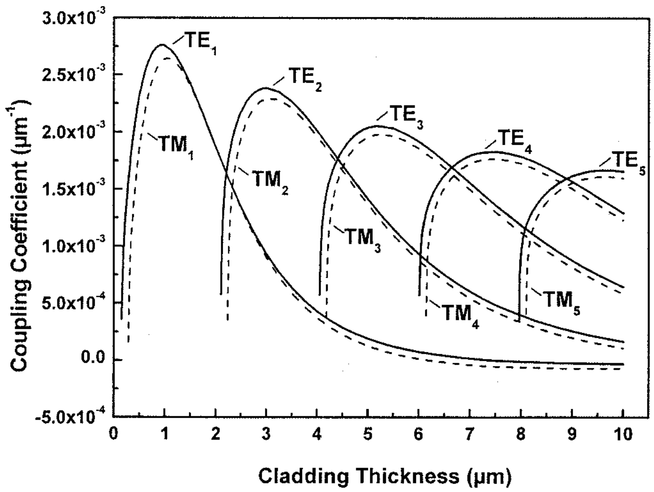

Fig. 4. Dependence of the coupling coefficients for several cladding modes on the cladding thickness d_{cl} for an LPWG with $n_s = 1.444$, $n_f = 1.53$, $n_{\text{cl}} = 1.50$, $n_{\text{cx}} = 1.0$, $d_f = 2.0\ \mu\text{m}$, $\Delta h = 0.1\ \mu\text{m}$, and $\lambda_0 = 1.584\ \mu\text{m}$.

V. Polarization-Independence Conditions

As shown by the results presented in the previous sections, the resonance wavelength and the coupling coefficient are in general sensitive to the polarization. It is possible, however, to obtain a polarization-independent resonance wavelength. The condition required is $D_m = 0$ ($m = 1, 2, \ldots$), where D_m is defined in (6). The dependence of D_1 on the cladding thickness d_{cl} is shown in Fig. 5(a) for three different wavelengths. At each wavelength, the value of D_1 can change from negative to positive as the cladding thickness increases. The value of d_{cl} required for achieving $D_1 = 0$ as a function of wavelength is

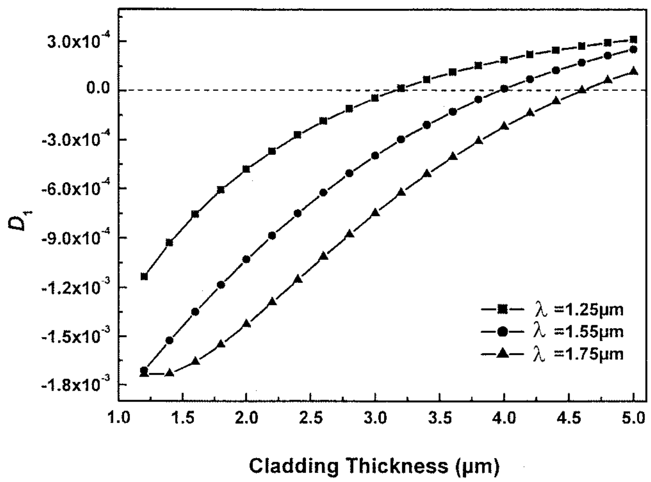

(a)

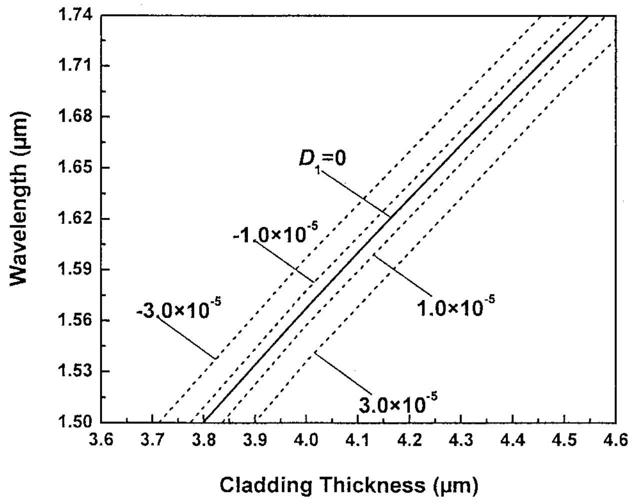

(b)

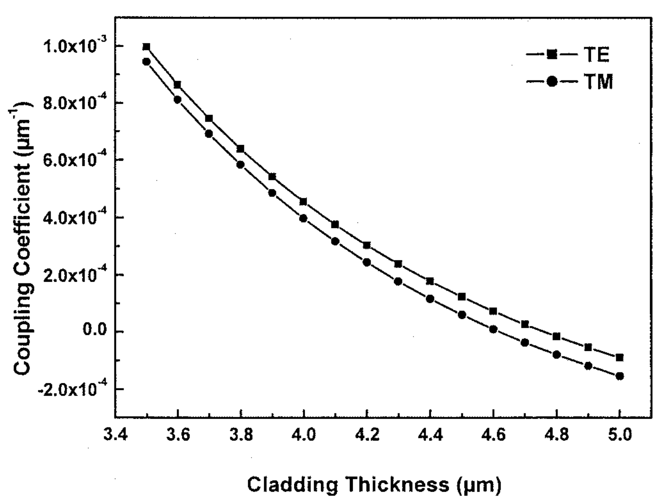

(c)

Fig. 5. (a) D_1 as a function of the cladding thickness $d_{\rm cl}$ at different wavelengths for a waveguide with $n_{\rm s} = 1.444$, $n_{\rm f} = 1.53$, $n_{\rm cl} = 1.50$, $n_{\rm cx} = 1.0$, and $d_{\rm f} = 2.0$ μm. (b) The cladding thickness $d_{\rm cl}$ required for achieving a specific value of D_1. (c) TE and TM coupling coefficients under the polarization-independence condition $D_1 = 0$.

shown in Fig. 5(b), and the corresponding coupling coefficients are shown in Fig. 5(c). Clearly, a proper choice of the cladding thickness can give the same resonance wavelength for both the TE and TM polarizations. For example, to obtain a polarization-independent resonance wavelength at 1.584 μm, we should use a cladding thickness of $d_{\rm cl} = 4.0$ μm. On the other hand, it seems impossible to equalize the coupling coefficients for the TE and TM polarizations. Fortunately, as shown in Fig. 5(c), the coupling coefficient depends weakly on the polarization. By carefully balancing the length of the grating and the corrugation depth, a polarization-independent coupling strength can be achieved. Being a periodic function of κ and L, the transmission coefficient given by (2) can attain the same value for two different values of κ. Because the coupling coefficients for the two polarizations are not too different, as shown in Fig. 4, the bandwidths of the rejection bands are expected to be insensitive to the polarization.

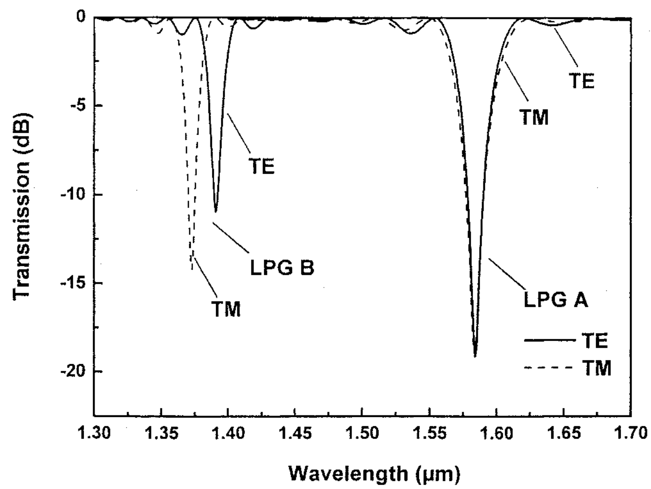

Fig. 6. Transmission spectra of two LPWGs with $n_{\rm s} = 1.444$, $n_{\rm f} = 1.53$, $n_{\rm cl} = 1.50$, $n_{\rm cx} = 1.0$, $d_{\rm f} = 2.0$ μm, $\Delta h = 0.1$ μm, $\Lambda = 70$ μm, and $L = 4$ mm, showing polarization-insensitive resonance at 1.584 μm for LPG A (with $d_{\rm cl} = 4.0$ μm) and two distinct resonance wavelengths for the two polarizations for LPG B (with $d_{\rm cl} = 5.0$ μm).

As an example, the transmission spectra of two LPWGs, LPG A and LPG B, are shown in Fig. 6, where $\Delta h = 0.1$ μm, $\Lambda = 70$ μm, $L = 4.0$ mm, and the TE_0–TE_1 and TM_0–TM_1 couplings are assumed. For LPG A, the cladding thickness is $d_{\rm cl} = 4.0$ μm, which is the value required for giving a polarization-independent resonance wavelength at 1.584 μm. For this grating, the coupling coefficients for the TE and TM polarizations are 4.31×10^{-4} μm^{-1} and 3.73×10^{-4} μm^{-1}, respectively, and the corresponding contrasts at the resonance wavelength are 19.1 and 19.0 dB. The bandwidths for the two polarizations are almost the same. On the other hand, for LPG B, the cladding thickness is $d_{\rm cl} = 5.0$ μm, which results in distinct rejection bands for the two polarizations, as shown in Fig. 6. While LPG A is useful for the construction of polarization-insensitive devices, LPG B can serve as a waveguide polarizer. For sensor applications, the two distinct bands in LPG B could be explored to overcome the problem of temperature interference by providing simultaneous measurement of temperature and the physical parameter of interest (e.g., the surrounding refractive index [18]).

The tolerance in the cladding thickness required for achieving a polarization-insensitive resonance wavelength is also shown in Fig. 5(b). It can be shown from the phase-matching condition that, with $\Lambda = 70\ \mu$m, $|D_1| = 1.0 \times 10^{-5}$ gives a difference in the resonance wavelength of ~0.7 nm between the two polarizations, which is small compared with the bandwidth of the rejection band. The corresponding tolerance in d_{cl} is $\sim 0.1\ \mu$m, which is well within the capacity of the modern waveguide fabrication technology.

VI. Conclusion

We have presented a detailed theoretical analysis of corrugated LPWGs in slab waveguides. We find that the cladding thickness of the waveguide has significant effects on the phase-matching curves, and as a result, an LPWG can produce phase-matching curves that are markedly different from those of an LPFG. Because the transmission spectrum and the sensitivity of the resonance wavelength to any physical parameter depend critically on such curves, an LPWG can show much richer characteristics than an LPFG. Further studies are being carried out to fully explore such characteristics. Our numerical results also confirm that corrugation is an effective means of introducing mode couplings, which means that a short corrugated LPWG is sufficient to produce a strong rejection band. Another distinct property of an LPWG is its polarization dependence. While both the resonance wavelength and the contrast of the rejection band are in general sensitive to the polarization of light, our results show the possibility of designing LPWGs with polarization-insensitive rejection bands. LPWG can be exploited as a flexible structure in the design of various kinds of wavelength-selective optical devices and sensors. Our theory can be extended to LPWGs in various kinds of rectangular-core waveguides by means of the effective-index method [26] or the perturbation method [27], which is a subject for further study. We expect more flexibility in the control of the polarization properties of LPWGs by adjustment of the dimensions of rectangular-core waveguides.

References

[1] A. M. Vengsarkar, P. J. Lemaire, J. B. Judkins, V. Bhatia, T. Erdogan, and J. E. Sipe, "Long-period fiber gratings as band-rejection filters," *J. Lightwave Technol.*, vol. 14, pp. 58–65, 1996.

[2] A. M. Vengsarkar, J. R. Pedrazzani, J. B. Judkins, P. J. Lemaire, N. S. Bergano, and C. R. Davidson, "Long-period fiber-grating-based gain equalizer," *Opt. Lett.*, vol. 21, pp. 336–338, 1996.

[3] J. R. Qian and H. F. Chen, "Gain flattening fiber filters using phase-shifted long period fiber gratings," *Electron. Lett.*, vol. 34, pp. 1132–1133, 1998.

[4] M. K. Pandit, K. S. Chiang, Z. H. Chen, and S. P. Li, "Tunable long-period fiber gratings for EDFA gain and ASE equalization," *Microwave Opt. Technol. Lett.*, vol. 25, pp. 181–184, 2000.

[5] X. J. Gu, "Wavelength-division multiplexing isolation fiber filter and light source using cascaded long-period fiber gratings," *Opt. Lett.*, vol. 23, pp. 509–510, 1998.

[6] K. S. Chiang, Y. Liu, M. N. Ng, and S. Li, "Coupling between two parallel long-period fiber gratings," *Electron. Lett.*, vol. 36, pp. 1408–1409, 2000.

[7] V. Bhatia and A. M. Vengsarkar, "Optical fiber long-period grating sensors," *Opt. Lett.*, vol. 21, pp. 692–694, 1996.

[8] H. J. Patrick, C. C. Chang, and S. T. Vohra, "Long period fiber gratings for structural bend sensing," *Electron. Lett.*, vol. 34, pp. 1773–1775, 1998.

[9] V. Grubsky and J. Feinberg, "Long-period fiber gratings with variable coupling for real-time sensing applications," *Opt. Lett.*, vol. 25, pp. 203–205, 2000.

[10] M. N. Ng, Z. Chen, and K. S. Chiang, "Temperature compensation of long-period fiber grating for refractive-index sensing with bending effect," *IEEE Photon. Technol. Lett.*, vol. 14, pp. 361–363, 2002.

[11] H. Jeong and K. Oh, "Theoretical analysis of cladding-mode waveguide dispersion and its effects on the spectra of long-period fiber grating," *J. Lightwave Technol.*, vol. 21, pp. 1838–1845, 2003.

[12] J. B. Judkins, J. R. Pedrazzani, D. J. DiGiovanni, and A. M. Vengsarkar, "Temperature-insensitive long-period fiber gratings," in *Tech. Dig. Optical Fiber Communication Conference (OFC'96)*, San Jose, CA, 1996, PD1.

[13] K. Shima, K. Himeno, T. Sakai, S. Okude, A. Wada, and R. Yamauchi, "A novel temperature-insensitive long-period fiber grating using a boron-codoped-germanosilicate-core fiber," in *Tech. Dig. Optical Fiber Communication Conference (OFC'97)*, Dallas, TX, 1997, FB2.

[14] A. A. Abramov, A. Hale, R. S. Windeler, and T. A. Strasser, "Widely tunable long-period fiber gratings," *Electron. Lett.*, vol. 35, pp. 81–82, 1999.

[15] X. Shu, T. Allsop, B. Gwandu, L. Zhang, and I. Bennion, "High-temperature sensitivity of long-period gratings in B-Ge codoped fiber," *IEEE Photon. Technol. Lett.*, vol. 13, pp. 818–820, 2001.

[16] S. Kim, Y. Jeong, S. Kim, J. Kwon, N. Park, and B. Lee, "Control of the characteristics of a long-period grating by cladding etching," *Appl. Opt.*, vol. 39, pp. 2038–2042, 2000.

[17] K. S. Chiang, Y. Liu, M. N. Ng, and X. Dong, "Analysis of etched long-period fiber grating and its response to external refractive index," *Electron. Lett.*, vol. 36, pp. 966–967, 2002.

[18] V. Rastogi and K. S. Chiang, "Long-period gratings in planar optical waveguides," *Appl. Opt.*, vol. 41, pp. 6351–6355, 2002.

[19] M. Kulishov, X. Daxhelet, M. Gaidi, and M. Chaker, "Electronically reconfigurable superimposed waveguide long-period gratings," *J. Opt. Soc. Amer. A*, vol. 19, pp. 1632–1648, 2002.

[20] K. S. Chiang, K. P. Lor, C. K. Chow, H. P. Chan, V. Rastogi, and Y. M. Chu, "Widely tunable long-period gratings fabricated in polymer-clad ion-exchanged glass waveguides," *IEEE Photon. Technol. Lett.*, vol. 15, pp. 1094–1096, 2003.

[21] H. Kogelnik, "Theory of optical waveguides," in *Guided-Wave Optoelectronics*, T. Tamir, Ed. Berlin: Springer-Verlag, 1990.

[22] M. J. Adams, *An Introduction to Optical Waveguides*. New York: Wiley, 1981, ch. 2.

[23] X. Shu, X. Zhu, Q. Wang, S. Jiang, W. Shi, Z. Huang, and D. Huang, "Dual resonant peaks of LP_{015} cladding mode in long-peirod gratings," *Electron. Lett.*, vol. 35, pp. 649–651, 1999.

[24] T. W. MacGougall, S. Pilevar, C. W. Haggans, and M. A. Jackson, "Generalized expression for the growth of long period gratings," *IEEE Photon. Technol. Lett.*, vol. 10, pp. 1449–1451, 1998.

[25] X. Shu, L. Zhang, and I. Bennion, "Sensitivity characteristics of long-period fiber gratings," *J. Lightwave Technol.*, vol. 20, pp. 255–266, 2002.

[26] K. S. Chiang, "Analysis of the effective-index method for the vector modes of rectangular-core dielectric waveguides," *IEEE Trans. Microwave Theory Tech.*, vol. 44, pp. 692–700, 1996.

[27] W. P. Wong and K. S. Chiang, "Design of polarization-insensitive Bragg gratings in zero-birefringence ridge waveguides," *IEEE J. Quantum Electron.*, vol. 37, pp. 1138–1145, 2001.

Qing Liu (S'03) received the B.S. and M.S. degrees in applied physics from Shanghai Jiao Tong University, China, in 1998 and 2001, respectively. He is currently pursuing the Ph.D degree in the Department of Electronic Engineering, City University of Hong Kong.

His research interests are mainly in the analysis and design of optical waveguides.

Kin Seng Chiang (M'94) received the B.E. (Hon.I) and Ph.D. degrees in electrical engineering from the University of New South Wales, Sydney, Australia, in 1982 and 1986, respectively.

In 1986, he spent six months in the Department of Mathematics, Australian Defence Force Academy, Canberra, Australia. From 1986 to 1993, he was with the Division of Applied Physics, Commonwealth Scientific and Industrial Research Organization (CSIRO), Sydney. From 1987 to 1988, he received a Japanese Government research award and spent six months at the Electrotechnical Laboratory, Tsukuba City, Japan. From 1992 to 1993, he worked concurrently for the Optical Fiber Technology Centre (OFTC) of the University of Sydney. In August 1993, he joined the Department of Electronic Engineering, City University of Hong Kong, where he is currently Chair Professor and Associate Head of the department. He has published more than 230 papers on optical fiber/waveguide theory and characterization, numerical methods, fiber devices and sensors, and nonlinear guided-wave optics.

Dr. Chiang is a Fellow of the Optical Society of America (OSA) and a Member of the International Society for Optical Engineering and the Australian Optical Society. He received the Croucher Senior Research Fellowship for 2000–2001.

Vipul Rastogi (M'00) received the B.Sc. degree from Rohilkhand University, Bareilly, India, in 1991, the M.Sc. degree from the Indian Institute of Technology Roorkee (formerly the University of Roorkee), India, in 1993, and the Ph.D. degree from the Indian Institute of Technology, Delhi, in 1998.

From 1998 to 1999, he was a Postdoctoral Fellow with Université de Nice Sophia-Antipolis, Nice, France. Since April 2000, he has been a Research Fellow in the Optoelectronics Research Centre, City University of Hong Kong. His research work has included second-order nonlinear interactions in optical waveguides, and periodically segmented waveguides. His current research interests are large mode area single-mode fibers, segmented cladding fibers, long-period waveguide gratings, and nonlinear directional couplers.

Dr. Rastogi is a Member of the the Optical Society of America (OSA).